**Proceedings of the ASME 2018 Conferences on Smart Materials, Adaptive Structures and Intelligent Systems**
**SMASIS 2018**
**September 10-12, 2018, San Antonio, USA**

**SMASIS2018-8203**

# SMART MATERIAL COMPOSITES FOR DISCRETE STIFFNESS MATERIALS

**Emily A Allen**
M3 Robotics Laboratory
School of Mechanical and Materials Engineering
Washington State University
Pullman, Washington, 99164
Email: emily.allen2@wsu.edu

**Lee D Taylor**
M3 Robotics Laboratory
School of Mechanical and Materials Engineering
Washington State University
Pullman, Washington, 99164
Email: lee.taylor@wsu.edu

**John P Swensen***
M3 Robotics Laboratory
School of Mechanical and Materials Engineering
Washington State University
Pullman, Washington, 99164
Email: john.swensen@wsu.edu

## ABSTRACT

*This paper presents an initial step towards a new class of soft robotics materials, where localized, geometric patterning of smart materials can exhibit discrete levels of stiffness through the combinations of smart materials used. This work is inspired by a variety of biological systems where actuation is accomplished by modulating the local stiffness in conjunction with muscle contractions. Whereas most biological systems use hydrostatic mechanisms to achieve stiffness variability, and many robotic systems have mimicked this mechanism, this work aims to use smart materials to achieve this stiffness variability. Here we present the compositing of the low melting point Field's metal, shape memory alloy Nitinol, and a low melting point thermoplastic Polycaprolactone (PCL), composited in simple beam structure within silicone rubber. The comparison in bending stiffnesses at different temperatures, which reside between the activation temperatures of the composited smart materials demonstrates the ability to achieve discrete levels of stiffnesses within the soft robotic tissue.*

## INTRODUCTION

Soft robotics and compliant robotic mechanisms have gained increasing popularity in the past decade within the academic community. This soft robotics approach is in stark contrast to the traditional paradigm of large, heavy, rapidly-moving robotics in isolated environments. The soft-robotic approach has shown promise because their compliant nature lends itself well to safety concerns in co-robotics environments and exhibits adaptability and robustness to uncertainty, such as in robotic grasping. However, this same intrinsic compliance in soft robotics is also its biggest pitfall — in many scenarios it is unable to exert necessary forces and control manipulator shape under external loading. However, biological systems abound where the primary method of actuation is the ability to adjust the stiffness of tissues in conjunction with localized muscle contractions. These type of actuation methods are widely prevalent in the muscular hydrostats, catch muscles, and catch connective tissues in cephalopods and echinoderms [1]. This combination of co-located muscle and adaptive tissue provide these animals with the ability to squeeze through holes much smaller than their average body diameter and capture or crush their prey. The primary focus of this paper is the development of new techniques in the compositing of existing soft-robotic technologies and carefully designed geometry of smart material additives to create robotic components with the ability to switch between acting as soft robotics or traditional rigid robotics, approaching the extreme capabilities of their biological counterparts, by presenting multiple discrete levels of stiffness.

Traditionally, robotic systems have followed the paradigm of being comprised primarily of rigid structures with relatively few degrees of freedom and well-characterized motion driven by actuators directly connected to the rigid links. In recent years, there

*Address all correspondence to this author.

 

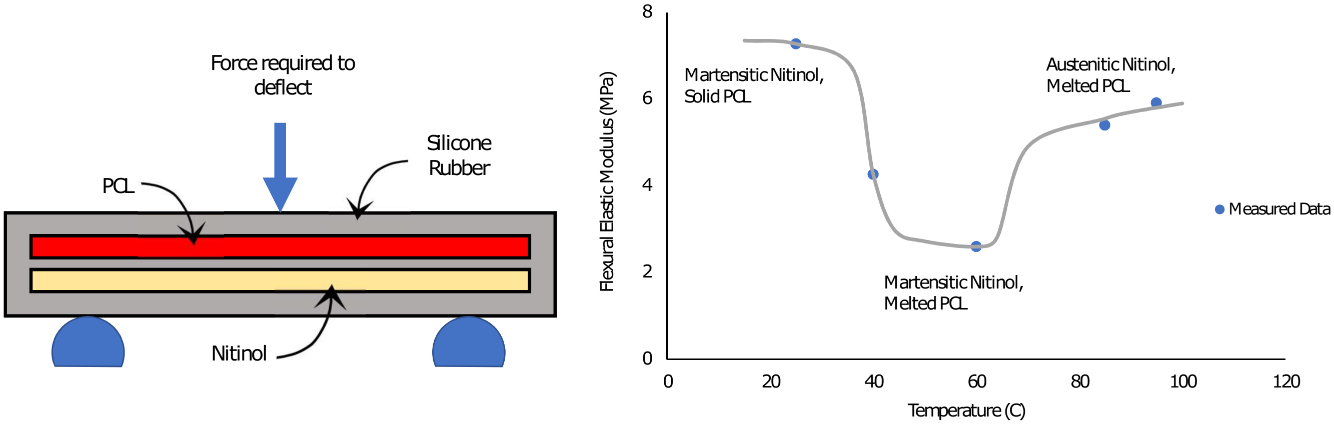


**FIGURE 1**. Three discrete stiffness levels achieved by composite of Nitinol and PCL rods encased in a silicone rubber matrix.

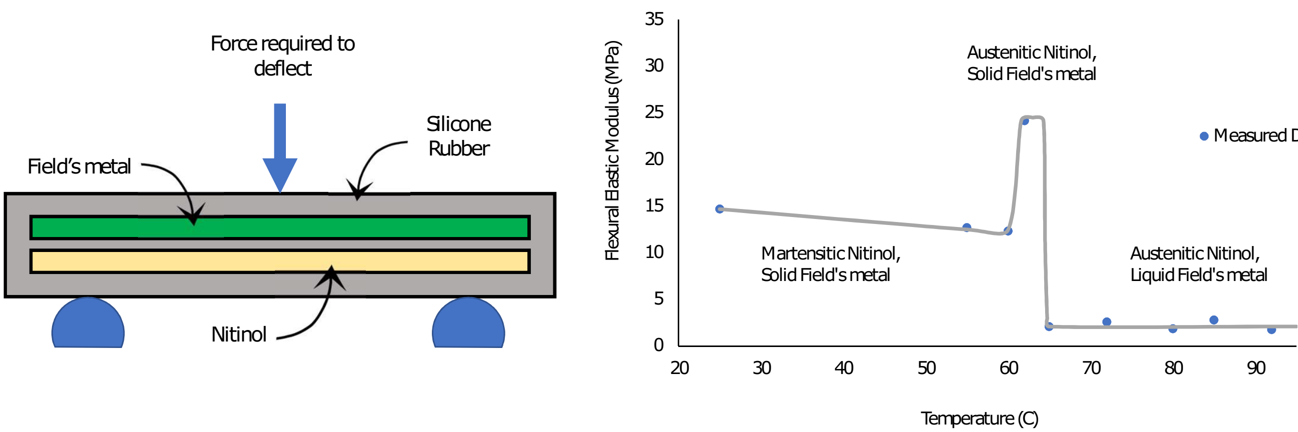


**FIGURE 2**. Three discrete stiffness levels achieved by composite of Nitinol and Field's metal rods encased in a silicone rubber matrix.

has been an explosion of research in the area of soft robotics, as they provide the promise of allowing robots and humans to work and collaborate in the same workspace. However, soft robotics have inherently limited ability to exert forces and interact with their surroundings in a meaningful way because of their compliant nature. Hence there is a great need for materials and mechanisms that have the ability to dynamically change between acting as a soft or a rigid robotic component.

**Variable stiffness actuators** Many variable stiffness actuators require complex design and machining to achieve a change of stiffness in even a single degree of freedom [2–4]. These often involve a high degree of complexity in terms of motors, mechanisms, and/or cable routings. Other approaches require high bandwidth feedback control to render a variable stiffness through a control system [5,6]. These approaches are usually not scalable and are more targeted at applications with a distinct drive train, rather than as material actuators and structures. However, when amenable these approaches provide the highest fidelity of rendered variable stiffness.

**Variable stiffness structures** Tensile integrity, or tensegrity, structures were initially used in architecture and artwork, with the term coined by Buckminster Fuller. It is characterized by systems of struts and cables where all of the cables have been prestressed and struts are either in compression or tension, thus maintaining the structural integrity of the whole. When applied to robotic systems, these tensegrity structures are designed such that the robot can selectively release tension in one or more cables, resulting in a predictable motion during collapse. Sequential loading and unloading of the cable generates reproducible gaits [7,8]. Other researchers are focusing on the valid tensegrity configurations that result in predictable deformations and their associated control [9,10].

**Soft Robotic Actuators** The majority of soft robotics, both actuators and systems, are primarily concerned with the problem of compliance matching to the task of the robotic system [11]. This is often accomplished through fabrication using purely elastomeric materials or with geometrically-complex chambers and pneumatic controls to deform an elastomer when the chambers are pressurized [12–14]. Previously, other geometric approaches to compliance were dominated by tendon driven robots with compliant backbones [15–18]. More recently, origami approaches to generating compliant mechanisms have also been employed [19].

Other recent efforts which are similar to the proposed work involve the combination of heaters and low-melting point metals, but these methods are restricted to a very thin geometry and global heating [20,21]. Other research using low melting point metals were focused on creating fabrics and threads with changeable stiffness [22,23]. The work presented in this paper is a first step towards the long term goal of stiffness control in magnitude, directionality, and spatial resolution. The focus is no longer just on the method of stiffening, as reviewed by Manti [24], but on how the compositing of multiple materials can result in multiple discrete stiffness levels within the same composite, as illustrated in Fig. 1 and Fig. 2.

## MATERIALS AND METHODS

Rods of Nitinol, PCL, and Fields metal are embedded in silicone rubber to form composite beams with variable stiffness due to the smart behavior of the constituent materials. 3-point bend tests are conducted on the composite beams and the individual materials at a range of temperatures spanning all three levels of discrete stiffness.

### Smart Materials

As shown in Table 1, each smart material used in this experiment exhibits a distinct change in stiffness at a specific critical temperature. This notable change in behavior can be explained by a change in microstructure or melting of the material. The critical temperatures and flexural modulus values listed in Table 1 were extracted from data from the 3-point bend test conducted on each material in this experiment.

**TABLE 1**. STIFFNESS VARIABILITY OF INDIVIDUAL SMART MATERIALS.

| Material | Critical temperature | Stiffness variability |
|---|---|---|
| Nitinol | 55 °C martensite to austenite | 21 GPa to 90 GPa |
| PCL | 58 °C melting temp (begins softening at lower temperatures) | 275 MPa to 0 MPa |
| Field's metal | 62 °C melting temp | 8.5 GPa to 0 GPa |

**Nitinol.** Nitinol is a nickel-titanium alloy that exhibits the shape-memory effect. Above the ciritcal temperature, the nitinol becomes austenitic, making it resistant to deformation. Below the critical temperature, this shape memory alloy transforms to a twinned martensite structure. Applying load to the material in its twinned martensite phase causes elastic deformation followed by de-twinning of the martensite. This de-twinning process results in pseudo-plastic deformation up to 7% strain. When the material is reheated above its critical temperature, it returns to its initial shape as it transforms to austenite. This unique behavior is desirable for variable stiffness composites as it offers high stiffness at high temperatures where most materials become softer or melt. Chemically pickled shape memory Nitinol wire from Confluent Medical (P/N WSM007500000SE) was used for this experiment. This particular wire was observed to transform from martensite to austenite between 45 and 60 °C.

**PCL.** Polycaprolactone (PCL) is a polyester that melts around 58 °C with a glass transition temperature of about -60 °C [25]. Unlike the instantaneous liquification of some materials, PCL softens gradually over a range of temperatures. It softens substantially before reaching its melting temperature, and even after melting completely, PCL remains extremely viscous. This transformation from a relatively rigid room temperature solid to a viscous melt at a slightly elevated temperature offers desirable behavior for varying stiffness at relatively low temperatures. FILAMENTS.CA's 2.85mm Low Temperature PCL Filament was used for this experiment.

**Field's metal.** Field's metal is a low melting-temperature eutectic alloy that melts uniformly at 62 °C. It is comprised of 51% indium, 32.5% bismuth, and 16.5% tin by weight. Field's metal is relatively soft compared to other metals with an elastic modulus only about an eighth that of aluminum at room temperature. It's low melting temperature lends itself to stiffness variability within a reasonable temperature range. Bismuth Indium Tin ingot Field's metal (stock number 46895) from Rotometals was used for this experiment.

### Test sample preparation

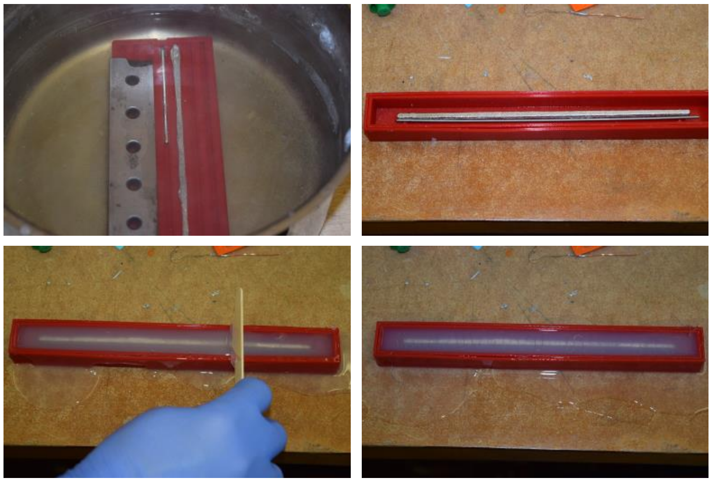

**FIGURE 3**. Preparation of the Nitinol/Field's metal composite. Field's metal casting (above left). Field's metal and Nitinol in mold (above right). Silicone is poured (bottom left). Nichrome heating element is submerged (bottom right).

To prepare the PCL-Nitinol samples used in these samples, six strands of 2.85mm diameter filament were cut to length, twisted around each other, and heated to a temperature of just over 60 °C using a hand held heat gun. The heated strands were when rolled by hand until the individual strands were not identifiable, and the nominal diameter was 4mm. The PCL bar and an identical length of 1.91mm diameter Nitinol were placed in a mold side by side, and a matrix of Smooth On$^{\mathrm{TM}}$ Dragon Skin 20 was poured into the top of the mold.

A nichrome heating element, used for bulk heating of the beam, was submerged into the top of the mold, to ensure no possibility of a short with the Nitinol. After the mold set, a type K thermocouple was embedded, positioned as close to the PCL and Nitinol as possible to provide representative measurements.

Preparation of the Field's metal rods for use in the Nitinol/Field's metal composite samples was completed using a mold submerged in water which was heated to a temperature just above the melting point of the Field's Metal. The process of creating the composite sample was otherwise identical to the PCL sample previously described.

Field's metal and PCL samples, intended for individual material testing, were created using the same methods layed out above, and were not enclosed in silicone. A silione-nichrome mold was cast for determining the properties of the matrix. A length of Nitinol was enclosed in a heat shrink exterior with a nichrome heating element wrapped around the outside, preventing a short through the Nitinol.

### Test processes

3-point bend tests were conducted on individual materials and composite beams using a Mark-10 Force Test Stand. As specified in the ISO standard for bend testing metallic materials, the equipment is fitted with polycarbonate supports and former of sufficient rigidity for this experiment [26]. The ASTM standard for bend testing plastic materials specifies a support span of 16 times the height of the testing specimen; the outer supports are spaced in conformance to the standard [27]. The polycarbonate loading nose attached to the load cell has a 10mm curvature radius to prevent the Nitinol from deforming at sharp, unrecoverable angles. The indenter was set to a travel speed of 5mm/s.

Each sample was tested up to 40mm center deflection to observe behavior under both plastic and elastic deformation. The sample temperature, monitored by a K-type thermocouple, was held constant throughout each test by toggling of the heating element. As recommended by ASTM, toe compensation was made to correct for the taking up of slack at the beginning of each test [27].

### Results and Discussion

Bend testing of the individual materials and composite beams revealed the stiffness variation and critical temperatures of each sample. The flexural elastic modulus is calculated from the equation

$$E = \frac{mL^3}{4wh^3} \tag{1}$$

for rectangular beams, or

$$E = \frac{4mL^3}{3\pi d^4} \tag{2}$$

for beams with round cross sections [27]. In both Eqs. 1 and 2, $m$ represents the slope of the initial linear region of the measured force-deflection curve; $L$ is the support span and $w$, $h$, and $d$ are the geometric dimensions of the specimens.

**Nitinol.** As seen in Figure 4, the force required to deform the pure Nitinol varies significantly with temperature. Although this overall material strength increases continuously with temperature, the elastic modulus of the Nitinol shown in Figure 5 exhibits two distinct levels of stiffness with a visible jump between the two levels at the transition from martensite to austenite. Most Nitinol transitions around 90°C, but the Nitinol wire used in this experiment transitions between 45 and 60°C ± 5°C.

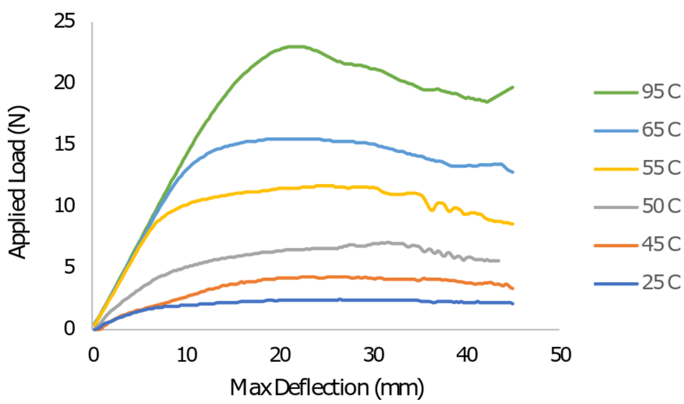


**FIGURE 4.** Measured load-deflection relationship for pure Nitinol rod at different temperatures.

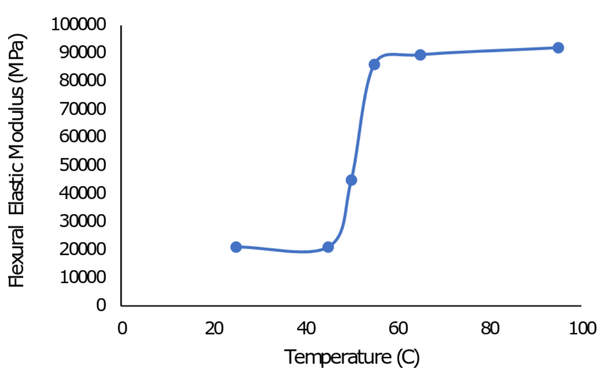


**FIGURE 5.** Measured flexural elastic modulus of pure Nitinol as a function of temperature.

**Silicone.** The Silicone rubber's contribution to the overall stiffness of the composite beams is minimal in comparison to the rigid smart materials, but its stiffness is analyzed experimentally nevertheless for the sake of improved accuracy. As seen from Figure 6, the silicone's stiffness remained constant at about 350 kPa across the measured range of temperatures. The minor deviations from the average stiffness can be explained by instrument uncertainties or slight initial sagging of the silicone between the outer supports.

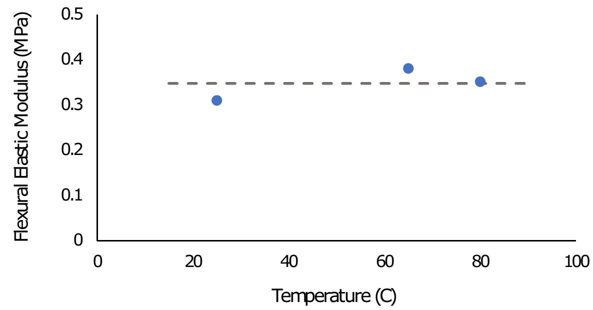


**FIGURE 6.** Measured flexural elastic modulus of pure Silicone rubber as a function of temperature.

**PCL.** The PCL rod became far less rigid at temperatures above room temperature. As seen in Figure 7, the material softened significantly even at just 30°C. The rod was observed to melt into a viscous liquid at about 60°C. Since a bend test cannot be conducted on a material in its liquid state, the flexural elastic modulus was assumed to be zero at temperatures above 60°C. A flexural modulus of 275 MPa was measured at 25°C. No measurements were taken below room temperature, but the stiffness is expected to plateau with only a slight increase at temperatures below 25°C.

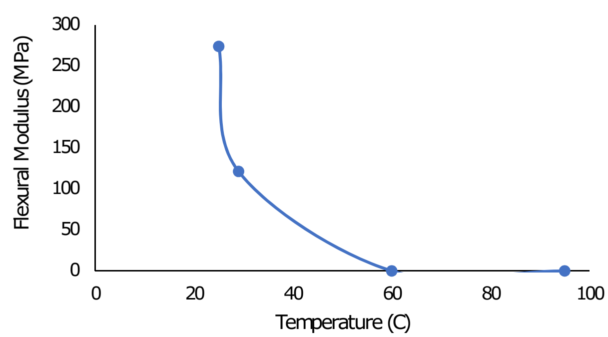


**FIGURE 7.** Measured flexural elastic modulus of pure PCL rod as a function of temperature.

**Field's metal.** The Field's metal exhibited typical eutectic behavior, showing a sharp melting point around 62 °C. At 25 °C, the Field's metal rod had a measured flexural elastic modulus of 8.45 GPa. This stiffness can be assumed to be nearly constant for temperatures between 0 and 62 °C when the metal is solid. At temperatures above 62 °C, the metal becomes liquid with an effective modulus of zero.

**Nitinol/PCL composite.** The combination of the smart behavior of Nitinol and PCL in the silicone rubber matrix results in a composite beam with unique, temperature-dependent properties. The beam stiffness is characterized by its flexural elastic modulus calculated from bend testing load-deflection data. As seen in Figure 1, three discrete stiffness levels were observed between temperatures of 25 and 100 °C.

The highest stiffness for this composite beam is achieved at temperatures below 40 °C, at which point the PCL is a rigid solid and the Nitinol is in its martensitic phase. In this region, the flexural elastic modulus was found to be 7.28 MPa when measured at 25 °C. Between 40 and 65 °C, the composite becomes flexible as the PCL melts. The Nitinol remains martensitic in this region, allowing large deformation as the microstructure transforms from twinned to de-twinned martensite. The modulus in this region was measured to be 2.60 MPa at 60 °C. At temperatures above 65 °C, the composite stiffens again as the PCL remains melted but the Nitinol transforms to austenite. In this medium-stiffness region, the average flexural modulus was found to be 5.65 MPa.

From the data collected from the composite beam, it is difficult to determine how rapidly the stiffness falls off as the PCL melts. However, the general shape of the curve may be inferred by observation of the softening and melting behavior of the pure PCL from in Figure 7. Since the Silicone and Nitinol exhibit constant stiffness at the range of temperatures over which the PCL softens and melts, the stiffness of the composite should decrease at the same rate as the stiffness of the pure PCL from Figure 7.

A unique twisting behavior was observed in the testing of the Nitinol/PCL composite above 60 °C. As evidenced in Figure 8, the composite twisted under the applied load of the bend test. At low temperatures, the parallel rods resist torsion, but above 60 °C, the PCL melts and provides no resistance to torsion in the composite beam. When applied to bulk materials, this feature could provide directional stability upon localized melting of specific PCL members.

**Nitinol/Field's metal composite.** The smart composite consisting of Nitinol and Field's metal rods in the silicone matrix also offers desirable stiffness variability. The Field's metal rod provides high stiffness at low temperatures while the Nitinol rod exhibits high stiffness at high temperatures. In a narrow band of mid-range temperatures, both materials provide high stiffness to the composite, causing very high stiffness at mid-range temperatures. The flexural elastic modulus for the composite was again gathered from load-deflection data over temperatures ranging from 25 to 95 °C.


**FIGURE 8**. Twisting behavior of Nitinol/PCL composite beam under loading of bend test above melting temperature of PCL.

At temperatures below 60 °C, the combination of the martensitic Nitinol and solid Field's metal produces the medium stiffness region seen on the left side of the plot in Figure 2 where the average modulus is 13.25 Mpa. The modulus spikes to 24.2 MPa over a narrow range of temperatures between about 60 and 63 °C where the Field's metal remains solid as the Nitinol becomes austenitic. The Field's metal then melts around 63 °C, causing a sharp drop in stiffness. The average flexural modulus is 2.22 MPa in this high-temperature region between 65 and 95 °C.

Some stiffness variation can be expected within each stiffness region as elastic modulus is known to decrease slightly with temperature for most materials. This slight decline can be seen in the low temperature region of the Nitinol/Field's metal composite shown in Figure 2. Fitting a curve to measured data allows for this factor to be easily accounted for when applying smart composites to specific applications. Alternatively, this slight variation may be neglected in some applications since it is relatively small compared to the large stiffness jumps at the critical temperatures.

## CONCLUSIONS AND FUTURE WORK

Composite beams were constructed with combinations of Nitinol/PCL and Nitinol/Field's metal rods positioned in parallel within a silicone matrix. The resulting composite stiffness was evidenced through a 3-point bend test conducted on the composite beam and its individual constituents at a range of temperatures from 25 to 95 °C. Three discrete stiffness levels were observed for each of the composite beams. Twisting behavior was observed in the case of the Nitinol/PCL composite as the PCL melted and allowed rotation about the Nitinol rod. Nearly constant stiffness was observed within each stiffness level wtih only a slight decrease with temperature as the stretching of the atomic bonds becomes easier. Heating of the Nitinol/PCL composite results in a high, low, medium stiffness sequence. The Nitinol/Field's metal composite exhibited medium, high, then low stiffness as temperature was increased.

In order to develop an effective system for controlling composite smart materials, it is necessary to develop an accurate model for the composite beam stiffness. Due to the smart behavior of each component and their inelastic behavior under large loads, the composite beam stiffness is a complicated function of both temperature and applied load. The melting and re-solidifying of the low melting temperature materials (PCL and Fields metal) further complicates the model. We seek to develop a model that characterizes the behavior of the two composite beams under various temperatures and applied loads.

Tests conducted for this paper examined the behavior of the materials and composites while held at constant temperatures. Further experimentation will be conducted to observe the effects of varying temperature during loading. The samples will be held at constant deflection within the elastic range while they are heated continuously. Continuous measurements of the sample temperature and force on the load cell will reveal a continuous relationship between the temperature and elastic modulus of the samples.

So far, the beams have not been retested after deformation of the Field's metal or PCL in their solid state. Repeated testing of the same specimens after melting and re-solidifying of the Field's metal and PCL will allow for characterization of this behavior.

In this experiment, tests were conducted on composite beams comprised of rods with one specific size and shape. However, customization of the stiffness in each temperature region may be achieved by modifying the geometry of the individual rods. This will alter the bending inertia of the individual materials and allow the magnitude of each discrete stiffness region to be customized to suit the relevant application. The temperature stimuli can also be shifted slightly by changing material compositions and alloying elements. Further research will explore the effects of extending the composite beam into 3 dimensions by testing the directional stiffness of composite truss structures.

## REFERENCES


[1] Schmidt-Nielsen, K., 1997. *Animal physiology: adaptation and environment*. Cambridge University Press.

[2] Tonietti, G., Schiavi, R., and Bicchi, A., 2005. "Design and control of a variable stiffness actuator for safe and fast physical human/robot interaction". In Robotics and Automation, 2005. ICRA 2005. Proceedings of the 2005 IEEE International Conference on, IEEE, pp. 526–531.

[3] Schiavi, R., Grioli, G., Sen, S., and Bicchi, A., 2008. "Vsa-ii: a novel prototype of variable stiffness actuator for safe and performing robots interacting with humans". In Robotics and Automation, 2008. ICRA 2008. IEEE International Conference on, IEEE, pp. 2171–2176.

[4] Tsagarakis, N. G., Sardellitti, I., and Caldwell, D. G., 2011. "A new variable stiffness actuator (compact-vsa): Design and modelling". In Intelligent Robots and Systems (IROS), 2011 IEEE/RSJ International Conference on, IEEE, pp. 378–383.

[5] Tagliamonte, N. L., Sergi, F., Accoto, D., Carpino, G., and Guglielmelli, E., 2012. "Double actuation architectures for rendering variable impedance in compliant robots: A review". *Mechatronics,* ***22***(8), pp. 1187–1203.

[6] Vanderborght, B., Albu-Schäffer, A., Bicchi, A., Burdet, E., Caldwell, D. G., Carloni, R., Catalano, M., Eiberger, O., Friedl, W., Ganesh, G., et al., 2013. "Variable impedance actuators: A review". *Robotics and autonomous systems,* ***61***(12), pp. 1601–1614.

[7] Paul, C., Roberts, J. W., Lipson, H., and Cuevas, F. V., 2005. "Gait production in a tensegrity based robot". In ICAR'05. Proceedings., 12th International Conference on Advanced Robotics, 2005., IEEE, pp. 216–222.

[8] Shibata, M., Saijyo, F., and Hirai, S., 2009. "Crawling by body deformation of tensegrity structure robots". In Robotics and Automation, 2009. ICRA'09. IEEE International Conference on, IEEE, pp. 4375–4380.

[9] Iscen, A., Agogino, A., SunSpiral, V., and Tumer, K., 2013. "Controlling tensegrity robots through evolution". In Proceedings of the 15th annual conference on Genetic and evolutionary computation, ACM, pp. 1293–1300.

[10] Paul, C., Valero-Cuevas, F. J., and Lipson, H., 2006. "Design and control of tensegrity robots for locomotion". *IEEE Transactions on Robotics,* ***22***(5), pp. 944–957.

[11] Majidi, C., 2014. "Soft robotics: a perspective–current trends and prospects for the future". *Soft Robotics,* ***1***(1), pp. 5–11.

[12] Daerden, F., and Lefeber, D., 2002. "Pneumatic artificial muscles: actuators for robotics and automation". *European journal of mechanical and environmental engineering,* ***47***(1), pp. 11–21.

[13] Trivedi, D., Rahn, C. D., Kier, W. M., and Walker, I. D., 2008. "Soft robotics: Biological inspiration, state of the art, and future research". *Applied Bionics and Biomechanics,* ***5***(3), pp. 99–117.

[14] Beyl, P., Van Damme, M., Van Ham, R., Vanderborght, B., and Lefeber, D., 2014. "Pleated pneumatic artificial muscle-based actuator system as a torque source for compliant lower limb exoskeletons". *Mechatronics, IEEE/ASME Transactions on,* ***19***(3), pp. 1046–1056.

[15] Li, C., and Rahn, C. D., 2002. "Design of continuous backbone, cable-driven robots". *Journal of Mechanical Design,*

***124***(2), pp. 265–271.

[16] Hannan, M. W., and Walker, I. D., 2003. "Kinematics and the implementation of an elephant's trunk manipulator and other continuum style robots". *Journal of Robotic Systems,* ***20***(2), pp. 45–63.

[17] Calisti, M., Giorelli, M., Levy, G., Mazzolai, B., Hochner, B., Laschi, C., and Dario, P., 2011. "An octopus-bioinspired solution to movement and manipulation for soft robots". *Bioinspiration & biomimetics,* ***6***(3), p. 036002.

[18] Laschi, C., Cianchetti, M., Mazzolai, B., Margheri, L., Follador, M., and Dario, P., 2012. "Soft robot arm inspired by the octopus". *Advanced Robotics,* ***26***(7), pp. 709–727.

[19] Vander Hoff, E., Jeong, D., and Lee, K., 2014. "Origamibot-i: A thread-actuated origami robot for manipulation and locomotion". In 2014 IEEE/RSJ International Conference on Intelligent Robots and Systems, IEEE, pp. 1421–1426.

[20] Shan, W., Lu, T., and Majidi, C., 2013. "Soft-matter composites with electrically tunable elastic rigidity". *Smart Materials and Structures,* ***22***(8), p. 085005.

[21] Wang, W., Rodrigue, H., and Ahn, S.-H., 2015. "Smart soft composite actuator with shape retention capability using embedded fusible alloy structures". *Composites Part B: Engineering,* ***78***, pp. 507–514.

[22] Chenal, T. P., Case, J. C., Paik, J., and Kramer, R. K., 2014. "Variable stiffness fabrics with embedded shape memory materials for wearable applications". In Intelligent Robots and Systems (IROS 2014), 2014 IEEE/RSJ International Conference on, IEEE, pp. 2827–2831.

[23] Shan, W., Diller, S., Tutcuoglu, A., and Majidi, C., 2015. "Rigidity-tuning conductive elastomer". *Smart Materials and Structures,* ***24***(6), p. 065001.

[24] Manti, M., Cacucciolo, V., and Cianchetti, M., 2016. "Stiffening in soft robotics: A review of the state of the art". *IEEE Robotics & Automation Magazine,* ***23***(3), pp. 93–106.

[25] *PCL Low Temperature Filament - Natural - 2.85mm*. See also URL https://filaments.ca/products/pcl-low-temperature-filament-natural-2-85mm.

[26] ISO 7438:2005(E), 2005. Metallic materials Bend test. Standard, International Organization for Standardization, Geneva, CH, June. See also URL http://allaboutmetallurgy.com/wp/wp-content/uploads/2016/12/ISO-7438.pdf.

[27] ATSM D790-03, 2003. Standard Test Methods for Flexural Properties of Unreinforced and Reinforced Plastics and Electrical Insulating Materials. Standard, ATSM International. See also URL http://mahshahr.aut.ac.ir/lib/exe/fetch.php?media=labs-astmd-790.pdf.